

EFFECTS CONTRIBUTING TO POSITIVE COOLANT VOID REACTIVITY IN CANDU¹

J.J. Whitlock^{a,c}, Wm.J. Garland^a, M.S. Milgram^b

^a McMaster University
Hamilton, Ontario, Canada

^b AECL
Chalk River, Ontario, Canada

^c *Current Address:*
AECL
Mississauga, Ontario, Canada

ABSTRACT

The lattice cell properties leading to positive coolant void reactivity in the CANDU reactor are described. The effect is subdivided into spectral, spatial, and isotopic components, and described in terms of criticality factors based on the six-factor formula for k_{eff} .

1. INTRODUCTION

The CANDU reactor is fuelled with natural uranium, and cooled and moderated by two separate D₂O circuits. The lattice cell is shown in Figure 1. The 37 fuel pins are surrounded by pressurized coolant at an average temperature of 290°C, and separated from the low-temperature moderator (average 70°C) by concentric fuel channel tubes and an insulating gap. The fuel pins are arranged in concentric rings of 1, 6, 12, and 18 pins, which will be referred to here as Ring 1, Ring 2, Ring 3, and Ring 4, respectively. The CANDU core is re-fuelled on-line, and therefore contains, after a period of initial re-fuelling has passed, fuel bundles at all stages of burnup.

This paper summarizes the neutronic components of coolant void reactivity in the CANDU lattice cell, measured in terms of the total effect,

$$\Delta\rho \equiv \rho(\text{voided}) - \rho(\text{cooled}) = \frac{k_{eff}(\text{voided}) - k_{eff}(\text{cooled})}{k_{eff}(\text{voided})k_{eff}(\text{cooled})} \times 1000 \text{ [mk]} \quad , \quad (1)$$

where "voided" and "cooled" refers to the absence and presence, respectively, of D₂O coolant.

¹ This material adapted from a Ph.D. thesis by J.J. Whitlock (Reference 3).
Phone number: (905)-823-9060 ext.4684; internet: whitlocj@candu.aecl.ca

The lattice cell code WIMS-AECL^{1,2} was used to model a typical CANDU lattice cell, using nominal geometric bucklings, the PIJ option (two-dimensional collision probabilities), and 69-group Winfrith library. The effect of cell voiding is modelled as a 100% instantaneous removal of coolant from the lattice. This is conservative due to the neglect of time-dependence and partial core voiding, considered more plausible in CANDU.

Spectral results are given in terms of "criticality factors"³, which are based on the common six-factor formula for k_{eff} . In this case results are grouped into three spectral groups: fast neutrons (0.821 MeV to 10 MeV), epithermal neutrons (0.625 eV to 0.821 MeV), and thermal neutrons (≤ 0.625 eV). The criticality factor formula is

$$k_{eff} = \eta f p_F p_E \epsilon \quad , \quad (2)$$

where η and f are the conventional "thermal yield efficiency" and "thermal utilization" terms, respectively, as applied to the thermal group defined above, ϵ is the fast-fission factor for the fast group defined above, and p_F and p_E are "escape-from-loss" terms for the fast and epithermal groups, respectively, as defined above. Leakage is included as an additional loss term in each of the f , p_F , and p_E components, which simplifies the analysis. Leakage from the CANDU core is a minor contributor to the reactivity of coolant voiding (adding a slightly negative component), and therefore neglecting its explicit treatment in this paper does not diminish the usefulness of the results.

Individual contributions from each of these criticality factors to the reactivity of coolant voiding can be found by substituting Equation (2) into Equation (1), and then using a multi-variable Taylor expansion to express $\Delta\rho$ as a sum of terms involving each of the criticality factors. In this manner the total effect can be analyzed as an exact linear sum of components.

Results are given at two different burnups, "zero-burnup" and "mid-burnup". The latter represents the half-way point of fuel residence, the resulting lattice cell calculation thus approximating the reactivity calculation of an equilibrium CANDU core with fuel bundles at all residence times.

2. NEUTRONIC ROLE OF COOLANT

The CANDU lattice cell contains 4% coolant and 83% moderator, by volume. Two distinct neutron sources result: a well-thermalized source within the moderator, and a fast source within the fuel. The void effect is related to the role that the coolant plays in inhibiting neutron transport between these two regions, a situation visualized in Figure 2. This inhibiting action is not directly in terms of absorption, since the coolant contributes only 0.03% to cell absorption, but in terms of scattering into the resonance region: down-scattering of fast neutrons and up-scattering of thermal neutrons.

Since the moderating property of the coolant is negligible compared to the bulk moderator, the net neutronic role of the coolant in the CANDU lattice is generally to decrease cell reactivity through increased resonance absorption, and decreased fast and thermal fission. The neutronic effect of voiding the coolant can be separated into spectral and spatial categories, described in Sections 3 and 4, respectively. In Section 5 the effect is described in relation to the main fissile isotopes of the fuel.

3. SPECTRAL COMPONENT OF COOLANT VOID REACTIVITY

Voiding of the coolant induces a spectral shift into both the fast and thermal regions, as shown in the plot of spectral change upon voiding in Figure 3. This result applies to the region of coolant surrounding the central fuel pin, representing the coolant location of maximum separation from the moderator. The burnup corresponding to the result in Figure 3 is mid-burnup, approximating conditions in an equilibrium core. Superimposed on Figure 3 are the main resonance regions, including that of the main plutonium isotopes. In fuel that is significantly irradiated, the presence of plutonium will lead to a reduction of the net reactivity upon voiding, because of the shift away from the large Pu-239 and Pu-241 fission resonance at about 0.3 eV. This situation is commented upon further in Section 5.

In Table 1 the spectral contributions to the total void effect ($\Delta\rho$) at both zero and mid-burnup are summarized in terms of the criticality factors described above. At zero-burnup the total effect is 16.3 mk, of which 31% (5.1 mk) is due to the thermal factors ($\eta+f$), 7% (1.2 mk) is due to the fast factors ($p_F+\epsilon$), and 62% (9.9 mk) is due to the epithermal factor (p_E).

At mid-burnup the presence of plutonium leads to a net negative contribution from the η component, and a reduction in the f component, which combine to reduce the total effect by 25% from its zero-burnup value. The thermal component of the total effect is actually zero due to a cancellation of the two contributing factors ($\eta+f$). The fast and epithermal contributions remain about the same (being largely due to U-238), but in terms of a relative contribution they are much larger since the thermal component is zero. At mid-burnup the fast contribution ($p_F+\epsilon$) is 15% of the total effect, while the epithermal portion (p_E) is 84%.

Clearly, resonance absorption plays the major role in the phenomenon of coolant void reactivity in the CANDU lattice.

4. SPATIAL COMPONENT OF COOLANT VOID REACTIVITY

The absence of up-scattering and an increase in streaming with coolant voiding affects a redistribution of thermal flux across the lattice cell, as illustrated in Figure 4. One way to demonstrate this change in transport properties is to compare the WIMS-AECL first-flight region-to-region collision probabilities (P_{ij}) before and after coolant voiding. Since the moderator is the effective bulk source of thermal neutrons, it is most relevant to compare the thermal group P_{ij} 's from the moderator to each of the four fuel rings. Table 2 makes this comparison by listing the ratios of P_{ij} (voided) to P_{ij} (cooled), where "i" is the moderator and "j" is each target fuel ring in turn. As expected, the greatest relative effect occurs between the moderator and the central fuel pin, decreasing with radius (and therefore proximity to the moderator). Note that these results reflect a change in probabilities, not actual events. Note also that these results reflect only the change in streaming properties since the "first-flight" collision probabilities are being utilized. They are still indicative of the total thermal effect however.

The redistribution of epithermal flux is illustrated in Figure 5. The epithermal flux decreases inside the pressure tube due to the loss of coolant as a high-end epithermal source. In the moderator the epithermal flux increases due to the increase in fast flux entering the moderator, and the corresponding increase in importance of the moderator as the sole thermalizing agent. The fast flux simply increases everywhere in the lattice cell due to spectral hardening, as illustrated in Figure 6.

The geometry-related effects of coolant voiding will create a varying spectral void effect across the lattice cell. Table 3 and Table 4 subdivide the void effect spectral components into separate fuel ring contributions, for zero-burnup and mid-burnup lattices, respectively. Results are given in both absolute terms (simple difference in the component's value) and relative terms (fractional change in the component's value). A special note must be made concerning the perturbation to the fast fission factor, ϵ , in this section on spatial dependence and the next on isotopic dependence. In these cases the "non-thermal fission" factor ϵ_{NT} is used, which describes the ratio of non-thermal to thermal fissions (as opposed to ϵ , the ratio of total fissions to thermal fissions). This notation provides more useful information by excluding the effects of large changes in the dominant thermal fission component. In the case of the U-238 contribution there is no difference between ϵ_{NT} and ϵ since it is not fissile in the thermal region.

In Table 3 and Table 4, the perturbations to both strictly thermal parameters, η and f , follow the same trend by fuel ring: the greatest relative increase is experienced in the inner fuel pin, decreasing with radial position and becoming negative in the outer fuel ring. This behaviour is not unexpected, based on the thermal flux spatial shift in Figure 4. With both thermal components the positive effect of the inner pins dominates in a zero-burnup lattice (Table 3) and the total contribution is positive. In a mid-burnup lattice (Table 4) the negative influence on η of plutonium in the outer pins leads to an overall negative change in this component (Section 5 illustrates this influence in more detail).

The perturbations to the non-thermal parameters, p_F , p_E and ϵ_{NT} , are determined largely by U-238 behaviour and are thus virtually independent of burnup. The greatest relative effects again occur in the inner fuel rings, although for all spectral components the greatest absolute perturbations occur in the outer fuel rings (as would be expected based on the trend of fuel volume with radius).

5. ISOTOPIC COMPONENTS OF COOLANT VOID REACTIVITY

The effect of coolant voiding can be further subdivided into the components attributable to each major nuclide in the fuel, U-235, U-238, and Pu-239. Such an analysis is given in Table 5 and Table 6 for the zero-burnup and mid-burnup lattices, respectively.

As Table 3 and Table 4 demonstrated, the general trend in the thermal range is for the greatest relative perturbation in criticality factors to occur near the centre of the fuel bundle, decreasing with radial position and becoming negative in the outer fuel region (Ring 4). In U-235 the negative shift of η and f in Ring 4 (caused by the negative shift in thermal flux here upon voiding) decreases with burnup due to depletion and competition for thermal absorption from burnup nuclides (fission products). The significant localized depletion in this area is illustrated in Table 7 comparing mid-burnup number densities by fuel ring, normalized to unity in the centre fuel pin in the case of U-235. Since the absolute perturbations to the U-235 thermal parameters in the inner fuel elements do not change as much with burnup as in the outer elements, the "outer ring effect" leads to an increase (about three-fold) in the thermal contribution of U-235 with burnup. This is evident when comparing the first two rows from the zero-burnup (Table 5) and mid-burnup (Table 6) results.

The major isotope of uranium, U-238, does not contribute to the perturbation in η since it does not produce thermal fissions, and therefore η is therefore not associated with U-238 in the two tables. U-238 does contribute about 34% of the thermal absorptions in a zero-burnup lattice and about 28% at mid-burnup. A significant portion of the increase in f upon voiding is therefore due to U-238, and this

contribution increases with burnup for the same reason as for U-235.

By mid-burnup, Pu-239 supplies about half the lattice cell fission yield and has a significant influence on the void effect. The bottom row in Table 7 compares the ring-by-ring concentration of Pu-239 in equilibrium fuel, normalized in this case to unity in the outer ring. Observe that the radial distribution of Pu-239 is somewhat "flatter" than that of U-235 at mid-burnup, caused by the greater geometric self-shielding across the bundle in the case of U-235 compared with U-238 (ie, the precursor to Pu-239). Nevertheless, the thermal void effect contribution of Pu-239 is still influenced by the radial dependence of thermal flux, as with U-235, and significant radial variation is again observed.

As mentioned earlier, plutonium has a negative influence on the void effect through the thermal parameters, caused by the shift of the equilibrium thermal spectrum away from plutonium's significant thermal fission resonance. It is important to note that the *isotopic* thermal yield/absorption ratio for Pu-239, for example, actually increases upon voiding, as shown in Table 8, which might lead to the conclusion of a *positive* influence on the void effect through the thermal parameters. This ratio, however, is not the same as plutonium's contribution to the thermal yield efficiency of the cell, η , and thus does not convey the same information. In this instance, although absorption in Pu-239 decreases upon voiding by a greater amount than yield, leading to positive values in Table 8, *total* cell absorption slightly increases, leading to negative values in Table 6. For completeness, the isotopic yield/absorption ratio for U-235 is also given in Table 8, and in Table 9 for a zero-burnup lattice. The total perturbation, in both cases, is positive (like Pu-239) but very small.

In the inner fuel rings the significant rise in thermal flux (see Figure 4) counters the negative influence of Pu-239 just described, leading to slightly positive perturbations in η and f in Table 6; the opposite is true for the outer rings where the decrease in thermal flux adds constructively to the negative spectral effect in plutonium. The overall effect is a combined thermal contribution that is strongly negative, reducing the total cell f parameter by a factor of five, and forcing the total cell η parameter significantly negative. The spatial "summary" of this information in Table 4 indicates that these two thermal effects effectively cancel each other.

Not surprisingly, the perturbations to the non-thermal parameters (p_F , p_E , and ϵ_{NT}) are almost exclusively attributable to U-238, and therefore independent of burnup. As Table 5 and Table 6 indicated, these perturbations, expressed in relative terms, are greatest near the centre of the cell and decrease slightly towards the outer fuel ring (also evident in the geometry effects given in Table 3 and Table 4). Again the exception is p_E , which shows a much steeper reduction in its positive perturbation near the outer fuel ring. In terms of absolute contributions, the most significant perturbation is to p_E for U-238, with about 80% of this occurring in the outer two fuel rings (see Table 5 and Table 6).

U-235 and Pu-239 make negligible contributions to the void effect through the non-thermal parameters, simply due to their low nuclide density. Note, however, that the relative perturbations to these parameters is comparable to U-238, with the notable exception that for both U-235 and Pu-239 the change in p_E is negative due to the dominance of their low-end epithermal absorption cross-sections. As indicated in Figure 3, this is a region of increasing flux with voiding.

The isotopic components as a function of burnup are plotted in Figure 1, which should be taken as an indicator of trend only since the environment surrounding a lattice cell actually contains fuel of all burnup stages. The point of mid-burnup is marked, and it is worth noting that the contributions from U-

238 and Pu-239 at this point cancel each other, making the U-235 contribution approximately equal to the total effect.

6. SUMMARY

The characteristics of the CANDU lattice with direct relevance to coolant void reactivity are: (1) the use of separate D₂O coolant and moderator with low absorption cross-section, (2) the large amount of moderator in the lattice, and (3) the very small ratio of coolant-to-moderator volume. The phenomena of coolant void reactivity has spatial, spectral, and isotopic dependence, and consists of many opposing constituent forces producing a net overall effect. The essential condition at the root of all else is the heterogeneous distribution of spectral sources within the lattice: high energy neutrons originating in the fuel region and low energy neutrons originating in the moderator region. The chief neutronic role of the coolant is to create an epithermal flux from these two sources, through down or up-scattering, and consequently the largest contributor to the void effect is a decrease in epithermal absorption. Smaller contributions come from the increase in fast fission and, in low-burnup cases, thermal utilization. In equilibrium or high burnup cases the presence of plutonium causes a net decrease with voiding of thermal utilization and fission neutrons per fuel absorption, leading to a lower void effect.

The voiding of coolant also affects a spatial redistribution of thermal flux, increasing in the centre region of the fuel bundle and decreasing in the outer region and moderator. In high burnup cases the decrease in the outer fuel region is a dominating negative influence on the void effect, acting mainly through the strong decrease in η for Pu-239. Countering this localized effect, the negative influence of U-235 in the outer fuel region decreases with burnup due to both depletion and absorption competition from fission products. At all burnup steps, however, the combined "outer ring" contribution of U-235 and Pu-239 to the void effect is significantly negative.

7. REFERENCES

1. J.V. Donnelly, *WIMS-CRNL: A User's Manual for the Chalk River Version of WIMS*, AECL-8955, AECL Research, 1986.
2. Griffiths, J., "WIMS-AECL Users Manual," AECL unpublished report, 1994.
3. Whitlock, J.J., "Reduction of the Coolant Void Reactivity Effect in a CANDU Lattice Cell", PhD Thesis, McMaster University, April 1995.

8. ACKNOWLEDGEMENT

This work was partially funded by the Natural Sciences and Engineering Research Council of Canada.

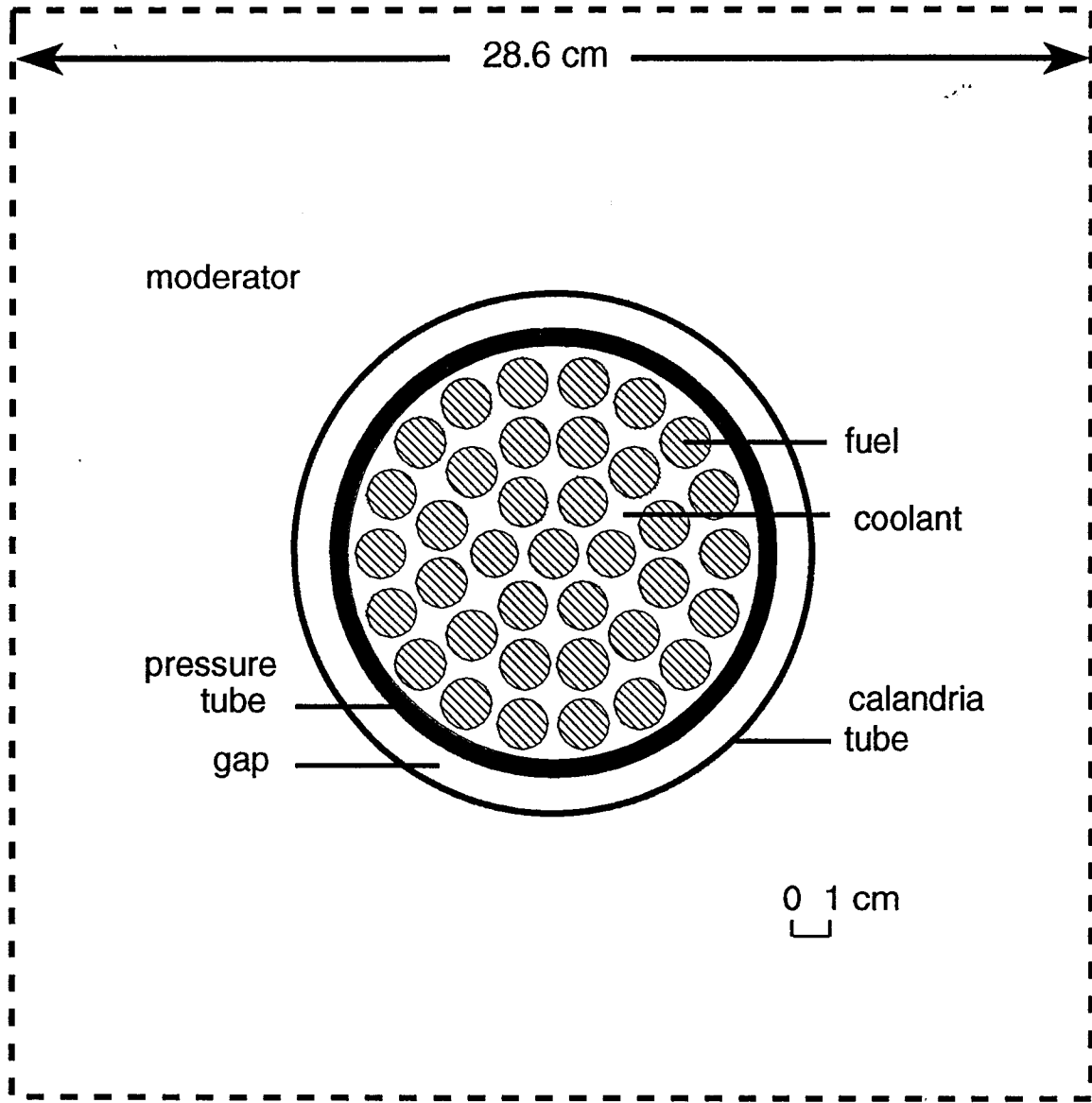


Figure 1. 37-Element CANDU Lattice Cell.

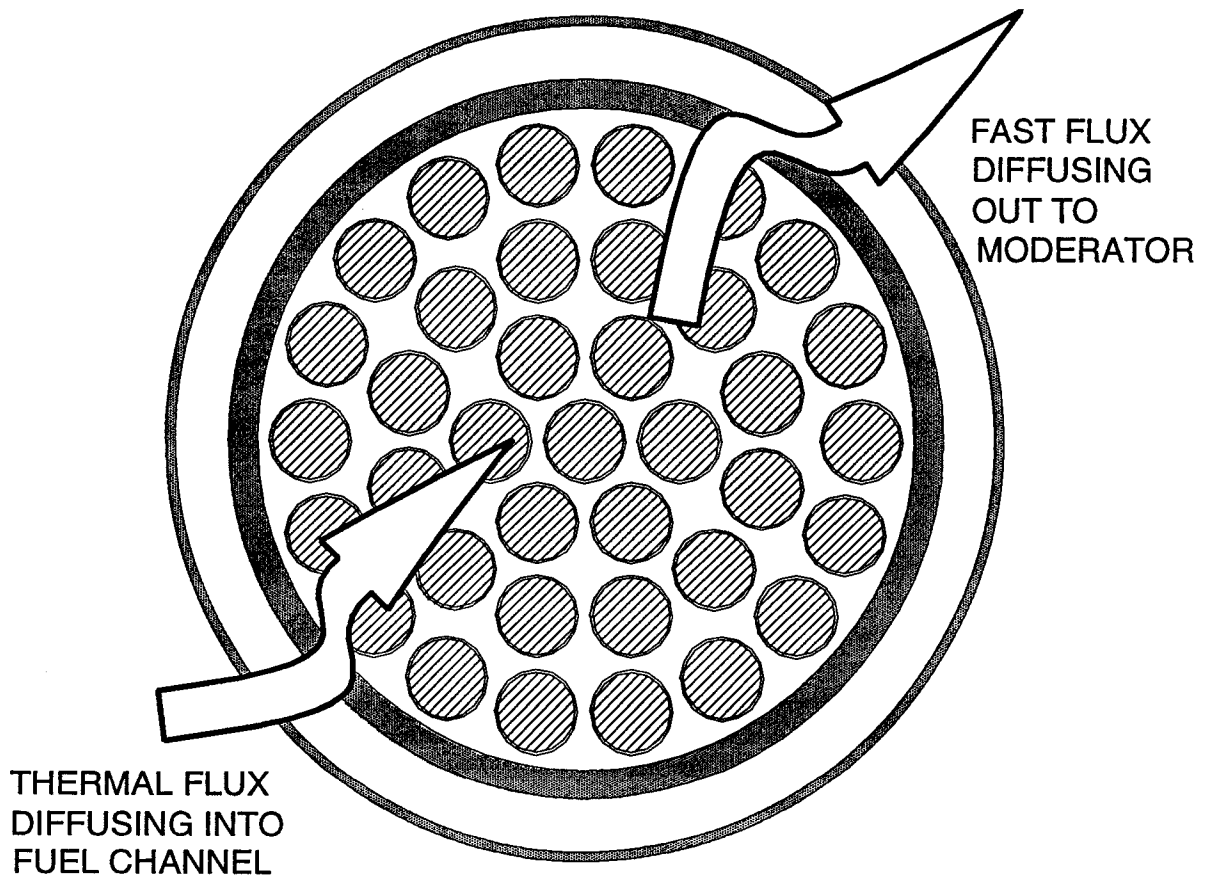


Figure 2. Concept of two distinct spectral sources in the CANDU lattice cell.

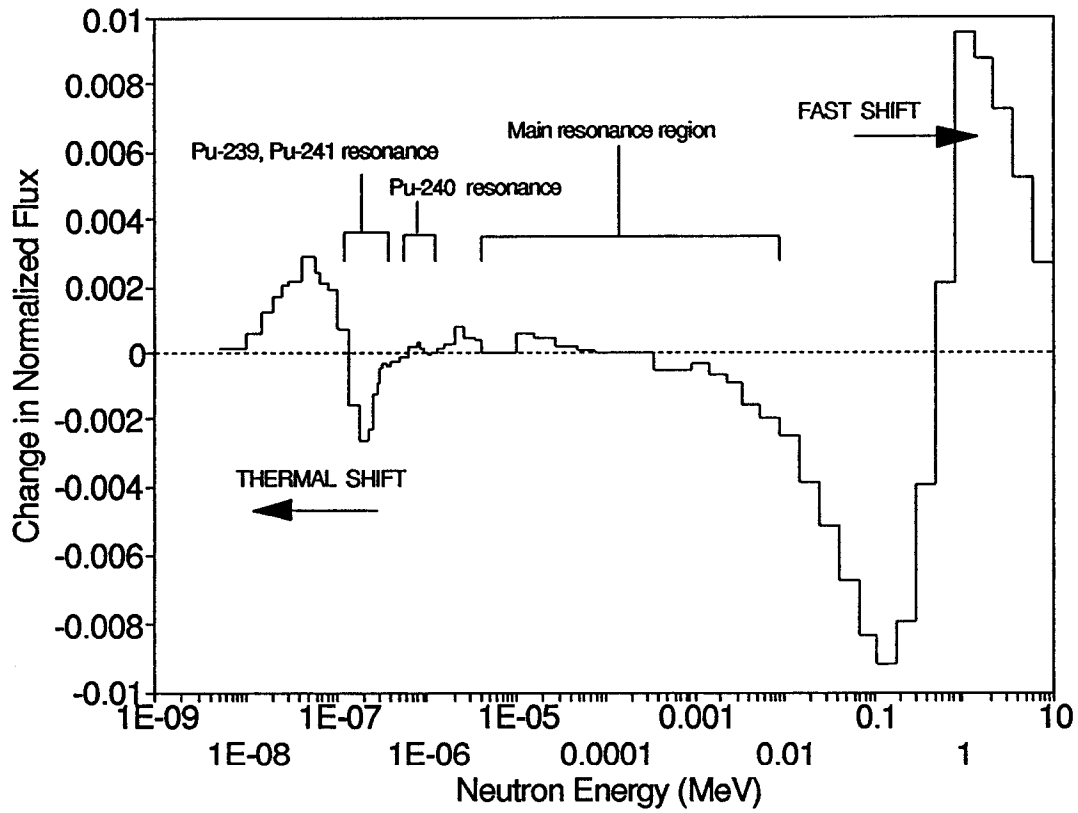


Figure 3. Change in Neutron Spectrum of Inner Coolant Region Upon Voiding: Mid-Burnup Lattice.

Table 1. Summary of Spectral Contributions to Total Void Effect in a Zero-Burnup and Mid-Burnup Lattice.

Criticality Factor	Value at Zero-Burnup (mk)	Value at Mid-Burnup (mk)
η	+1.8	-2.1
f	+3.3	+2.0
ρ_F	-3.2	-3.4
ρ_E	+9.9	+10.9
ϵ	+4.4	+5.4
TOTAL EFFECT	+16.3	+13.0

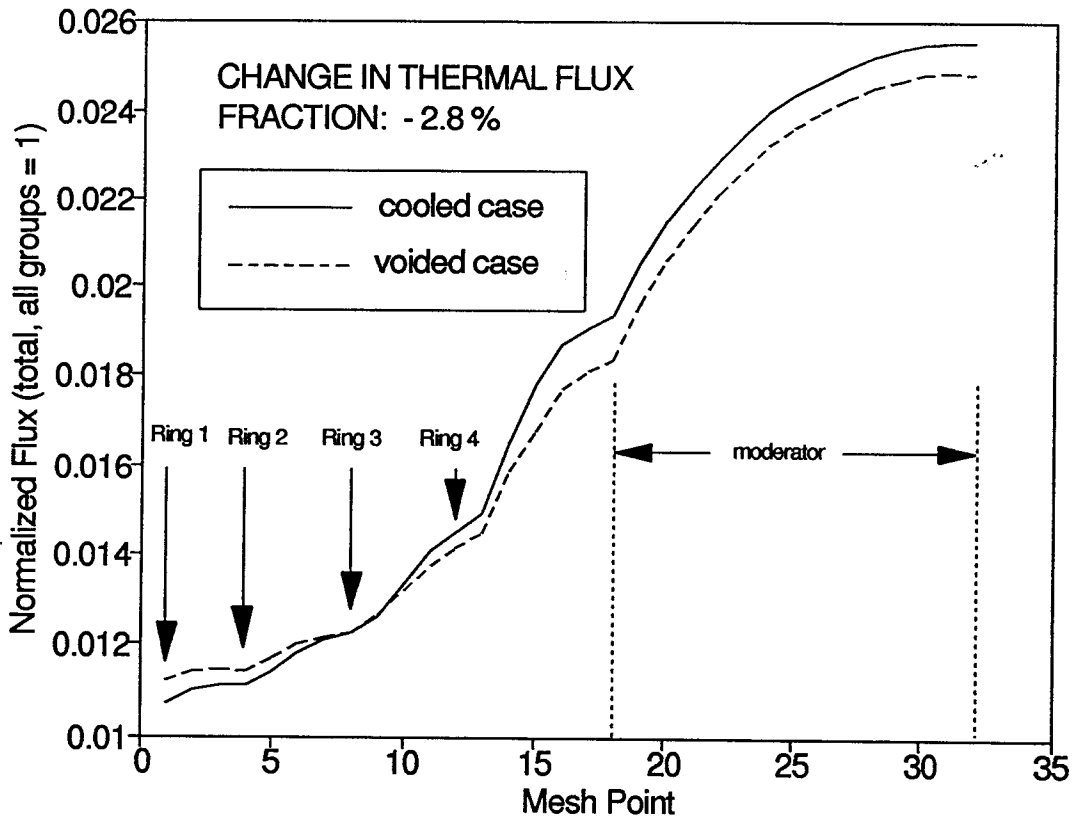


Figure 4 Normalized Spatial Distribution of Thermal Flux Across Mid-Burnup CANDU Lattice Cell for Cooled and Voided Cases.

Table 2 Ratio of Average Thermal Group Moderator-to-Fuel Collision Probabilities: P_{ij} (voided) / P_{ij} (cooled).

Target Fuel Ring	Ring 1	Ring 2	Ring 3	Ring 4
Ratio	2.0	1.8	1.6	1.3

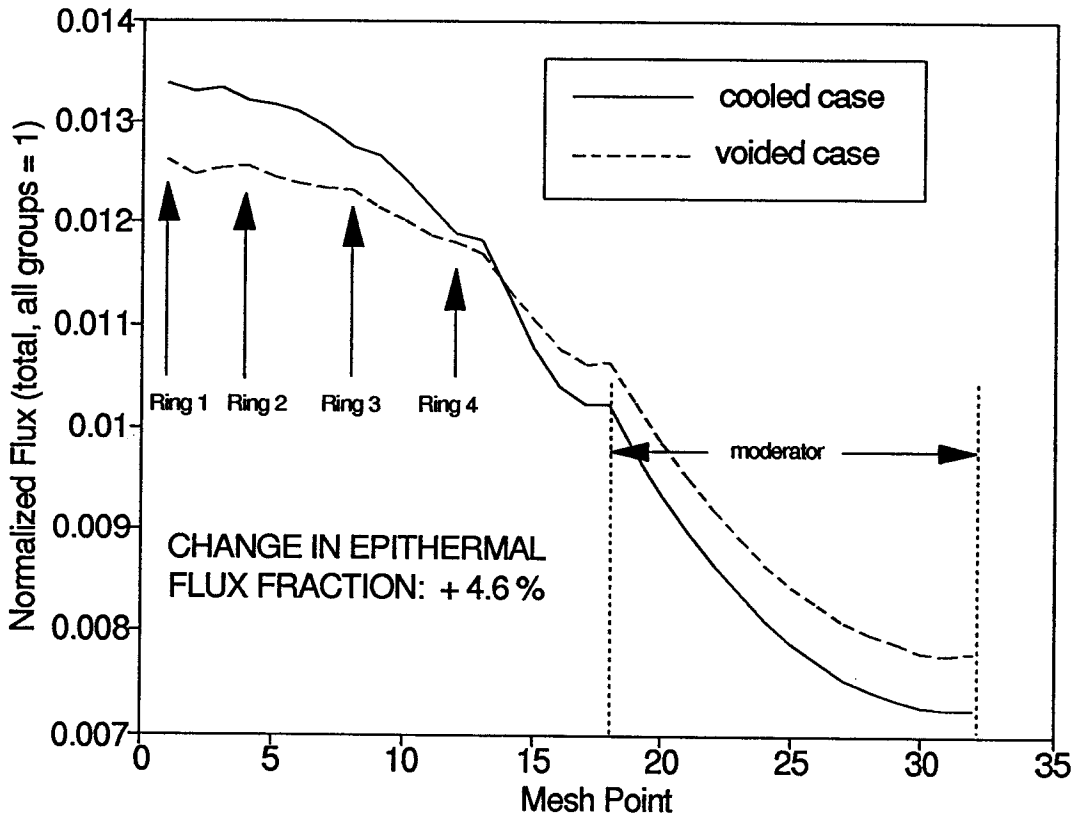


Figure 5 Normalized Spatial Distribution of Epithermal Flux Across Mid-Burnup CANDU Lattice Cell for Cooled and Voided Cases.

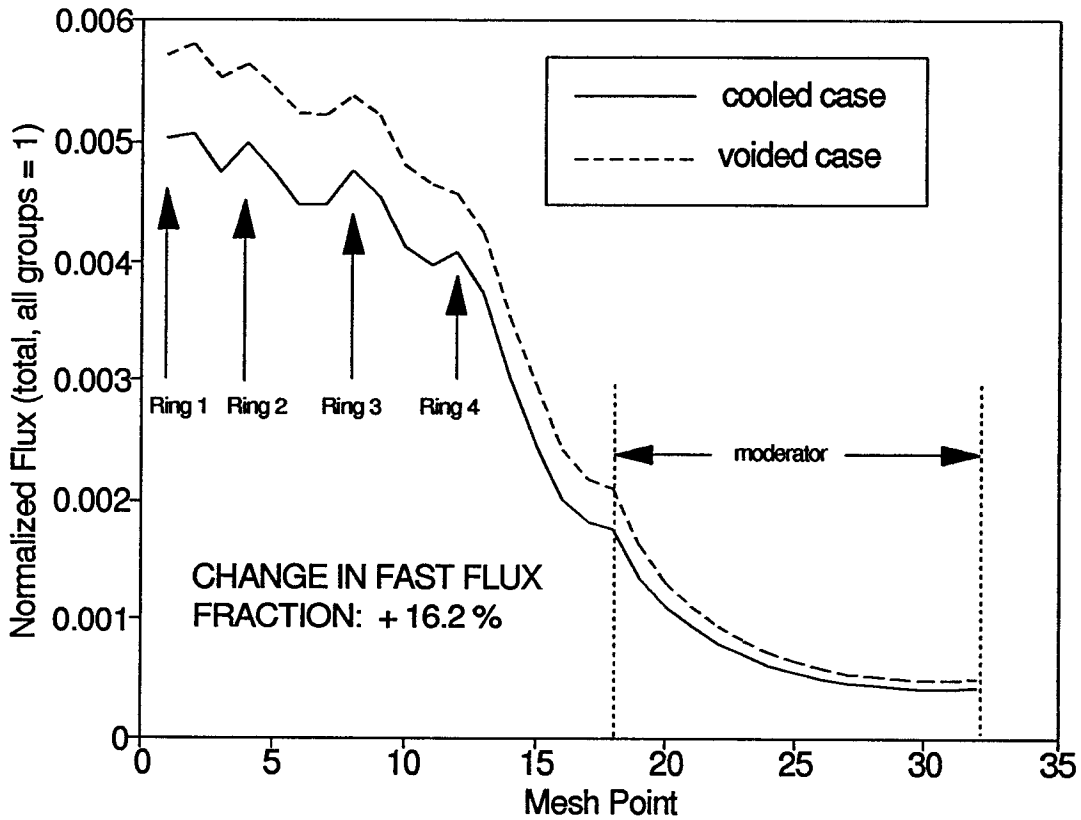


Figure 6 Normalized Spatial Distribution of Fast Flux Across Mid-Burnup CANDU Lattice Cell for Cooled and Voided Cases.

Table 3 Fuel Ring Contributions (Absolute and Relative) to Change in Criticality Factors Upon Voiding in a Zero-Burnup Lattice.

Criticality Factor	Change in Component Upon Voiding					
	type	Ring 1	Ring 2	Ring 3	Ring 4	TOTAL
η	abs.	.0021	.0084	.0079	-.0158	.0026
	rel.	7.8 %	5.0 %	2.1 %	-2.2 %	0.3 %
f	abs.	.0015	.0060	.0059	-.0101	.0034
	res.	7.7 %	5.0 %	2.2 %	-2.0 %	0.4 %
ρ_F	abs.	-.0001	-.0005	-.0009	-.0011	-.0026
	rel.	-11.5 %	-11.4 %	-10.6 %	-9.8 %	-10.4 %
ρ_E	abs.	.0003	.0020	.0040	.0037	.0100
	rel.	10.5 %	10.5 %	10.1 %	5.4 %	7.7 %
ϵ_{NT}	abs.	.0002	.0010	.0018	.0021	.0050
	rel.	7.1 %	6.9 %	6.1 %	5.3 %	5.9 %

Table 4 Fuel Ring Contributions (Absolute and Relative) to Change in Criticality Factors Upon Voiding in a Mid-Burnup Lattice.

Criticality Factor	Change in Component Upon Voiding					
	type	Ring 1	Ring 2	Ring 3	Ring 4	TOTAL
η	abs.	.0021	.0082	.0063	-.0196	-.0029
	rel.	7.7 %	4.7 %	1.6 %	-2.6 %	-0.3 %
f	abs.	.0016	.0064	.0059	-.0113	.0026
	rel.	8.3 %	5.4 %	2.2 %	-2.2 %	0.3 %
ρ_F	abs.	-.0001	-.0005	-.0009	-.0011	-.0026
	rel.	-11.6 %	-11.5 %	-10.7 %	-9.8 %	-10.5 %
ρ_E	abs.	.0003	.0021	.0041	.0038	.0103
	rel.	10.2 %	10.2 %	9.7 %	5.1 %	7.3 %
ϵ_{NT}	abs.	.0002	.0012	.0020	.0025	.0059
	rel.	7.9 %	7.7 %	7.0 %	6.2 %	6.8 %

Table 5 Material Contributions by Location (Absolute and Relative) to Change in Criticality Factors Upon Voiding in a Zero-Burnup Lattice.

Material	Criticality Factor	Change in Component Upon Voiding*					
		type	Ring 1	Ring 2	Ring 3	Ring 4	TOTAL
U-235	η	abs.	.0021	.0084	.0079	-.0154	.0030
		rel.	7.8 %	5.0 %	2.1 %	-2.2 %	0.3 %
	f	abs.	.0009	.0039	.0040	-.0060	.0028
		rel.	8.0 %	5.2 %	2.3 %	-1.9 %	0.5 %
	ρ_F	abs.	.0000	.0000	.0000	.0000	-.0001
rel.		-12.5 %	-12.5 %	-11.8 %	-11.1 %	-11.6 %	
ρ_E	abs.	.0000	.0000	-.0001	-.0002	-.0003	
	rel.	-1.8 %	-1.5 %	-1.4 %	-2.0 %	-1.7 %	
ϵ_{NT}	abs.	.0000	.0000	.0000	.0001	.0002	
	rel.	0.8 %	0.5 %	0.4 %	0.8 %	0.6 %	
U-238	f	abs.	.0005	.0021	.0019	-.0040	.0005
		rel.	7.3 %	4.7 %	1.9 %	-2.1 %	0.2 %
	ρ_F	abs.	-.0001	-.0005	-.0009	-.0011	-.0025
		rel.	-11.7 %	-11.6 %	-10.8 %	-10.0 %	-10.6 %
ρ_E	abs.	.0003	.0021	.0041	.0039	.0105	
	rel.	12.3 %	12.3 %	11.8 %	6.4 %	9.0 %	
ϵ_{NT}	abs.	.0002	.0010	.0018	.0021	.0051	
	rel.	9.7 %	9.6 %	8.7 %	7.8 %	8.5 %	

* Zero entry indicates negligible result.

Table 6 Material Contributions by Location (Abs. and Rel.) to Change in Criticality Factors Upon Voiding in a Mid-Burnup Lattice.

Material	Criticality Factor	Change in Component Upon Voiding*					
		type	Ring 1	Ring 2	Ring 3	Ring 4	TOTAL
U-235	η	abs.	.0016	.0070	.0080	-.0038	.0128
		rel.	11.0 %	7.6 %	3.9 %	-1.1 %	2.0 %
	f	abs.	.0007	.0029	.0034	-.0013	.0057
		rel.	11.1 %	7.7 %	4.1 %	-1.0 %	2.1 %
	ρ_F	abs.	.0000	.0000	.0000	.0000	.0000
rel.		-12.5 %	-12.6 %	-11.8 %	-11.1 %	-11.7 %	
ρ_E	abs.	.0000	.0000	.0000	-.0001	-.0001	
	rel.	-1.3 %	-0.9 %	-0.8 %	-1.8 %	-1.3 %	
ϵ_{NT}	abs.	.0000	.0000	.0000	.0001	.0001	
	rel.	0.6 %	0.3 %	0.3 %	1.0 %	0.6 %	
U-238	f	abs.	.0006	.0025	.0030	-.0019	.0042
		rel.	10.4 %	7.1 %	3.6 %	-1.2 %	1.5 %
	ρ_F	abs.	-.0001	-.0005	-.0009	-.0011	-.0025
		rel.	-11.8 %	-11.7 %	-10.9 %	-10.0 %	-10.7 %
ρ_E	abs.	.0004	.0021	.0042	.0040	.0106	
	rel.	12.7 %	12.6 %	12.1 %	6.6 %	9.3 %	
ϵ_{NT}	abs.	.0002	.0011	.0020	.0024	.0057	
	rel.	10.3 %	10.2 %	9.3 %	8.4 %	9.1 %	
Pu-239	η	abs.	.0005	.0011	-.0017	-.0151	-.0153
		rel.	3.7 %	1.4 %	-0.9 %	-3.9 %	-2.3 %
	f	abs.	.0002	.0002	-.0012	-.0071	-.0080
		rel.	2.8 %	0.6 %	-1.5 %	-4.2 %	-2.7 %
	ρ_F	abs.	.0000	.0000	.0000	.0000	.0000
rel.		-12.5 %	-12.5 %	-11.7 %	-11.0 %	-11.5 %	
ρ_E	abs.	.0000	.0000	.0000	-.0001	-.0001	
	rel.	-3.8 %	-3.3 %	-3.0 %	-2.6 %	-2.9 %	
ϵ_{NT}	abs.	.0000	.0000	.0001	.0001	.0002	
	rel.	3.3 %	1.6 %	2.6 %	2.2 %	2.4 %	

* Zero entry indicates negligible result.

Table 7 Relative Fuel Ring Nuclide Densities for U-235 and Pu-239 in a Mid-Burnup Lattice (Separate Normalization).

Nuclide	Ring 1	Ring 2	Ring 3	Ring 4
U-235	1	0.98	0.92	0.79
Pu-239	0.83	0.84	0.89	1

Table 8 Change in Thermal Yield/Absorption Ratio of U-235 and Pu-239, by Location, Upon Voiding in a Mid-Burnup Lattice.

Material	Ring 1	Ring 2	Ring 3	Ring 4	TOTAL
U-235	+0.3 %	+0.2 %	+0.2 %	+0.1 %	+0.2 %
Pu-239	+2.2 %	+1.9 %	+1.6 %	+1.0 %	+1.3 %

Table 9 Change in Thermal Yield/Absorption Ratio of U-235, by Location, Upon Voiding in a Zero-Burnup Lattice.

Material	Ring 1	Ring 2	Ring 3	Ring 4	TOTAL
U-235	+0.3 %	+0.3 %	+0.2 %	+0.1 %	+0.2 %

Table 10 Contribution (in mk) of Fissile Materials to Void Reactivity Effect Through Change in Neutron Yield in a Zero-Burnup Lattice.

Material	Energy Group	Contribution to $\Delta\rho_v$ through yield (mk)				
		Ring 1	Ring 2	Ring 3	Ring 4	TOTAL
U-235	fast	0.0	0.0	0.0	0.1	0.1
	epithermal	0.0	0.0	0.1	0.2	0.3
	thermal	1.5	6.8	7.7	-5.1	10.9
	TOTAL	1.5	6.8	7.8	-4.8	11.3
U-238	fast	0.2	1.0	1.7	2.1	5.0
	epithermal	0.0	0.0	0.0	0.0	0.0
	thermal	0.0	0.0	0.0	0.0	0.0
	TOTAL	0.2	1.0	1.7	2.1	5.0
Total Effect:					16.3	

Table 11 Contribution (in mk) of Fissile Materials to Void Reactivity Effect Through Change in Neutron Yield in a Mid-Burnup Lattice.

Material	Energy Group	Contribution to $\Delta\rho_v$ through yield (mk)				
		Ring 1	Ring 2	Ring 3	Ring 4	TOTAL
U-235	fast	0.0	0.0	0.0	0.0	0.0
	epithermal	0.0	0.0	0.0	0.1	0.1
	thermal	1.2	5.5	6.8	-0.3	13.2
	TOTAL	1.2	5.5	6.8	-0.2	13.3
U-238	fast	0.2	1.2	2.0	2.3	5.7
	epithermal	0.0	0.0	0.0	0.0	0.0
	thermal	0.0	0.0	0.0	0.0	0.0
	TOTAL	0.2	1.2	2.0	2.3	5.7
Pu-239	fast	0.0	0.0	0.0	0.0	0.0
	epithermal	0.0	0.0	0.1	0.1	0.2
	thermal	0.4	1.3	0.1	-8.0	-6.2
	TOTAL	0.4	1.3	0.2	-7.8	-6.0
Total Effect:					13.0	

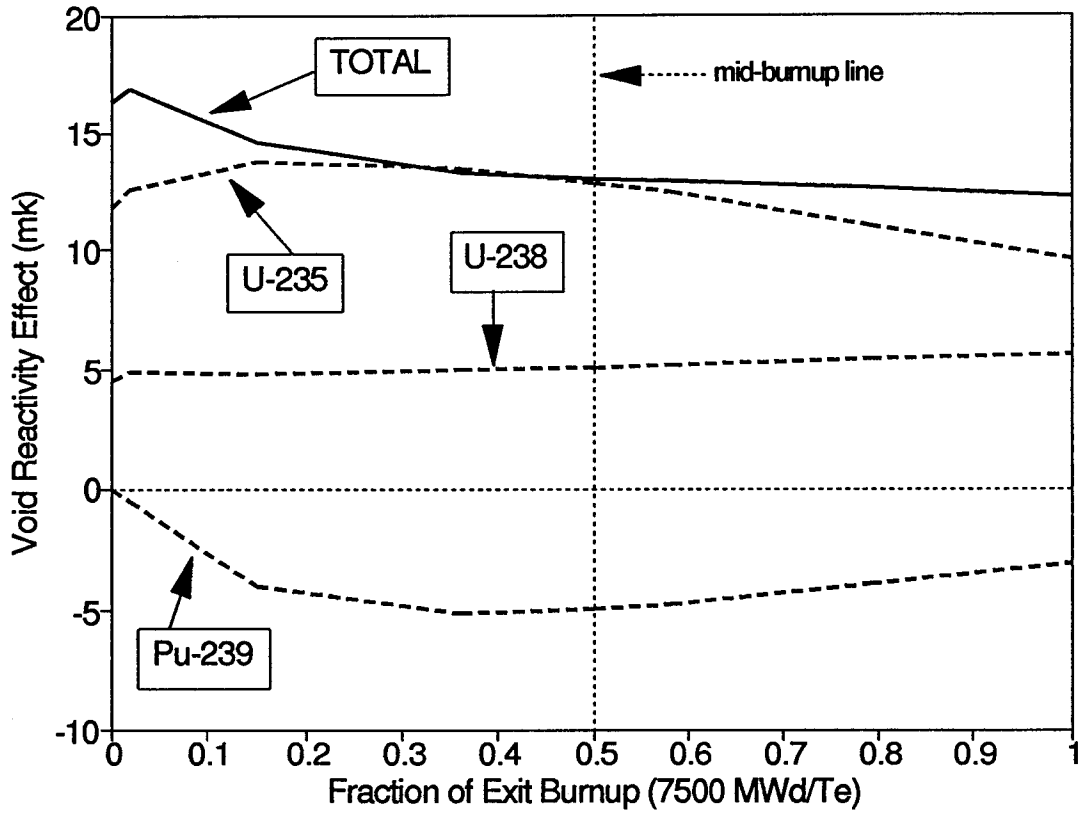


Figure 1 Contribution of Fissile Material to Void Reactivity Effect Through Change in Neutron Yield vs. Burnup Fraction.